Development of Fast Large Lead-Acid Battery Charging System Using Multi-state Strategy

Cheng Siong Lee[1], Hsiung Cheng Lin [2] and Sin-You Lai [2]

Abstract

Currently, there are many kinds of batteries available for primary or backup power sources. Among them, applications of acid battery is one of most important devices due to low cost and continuously improving battery technology. However, a well optimized charging process usually requires a complex control circuitry, such as microprocessors, DSP chips or other power electronics controllers. This paper proposes a fast multi-state charging system with UC3906, particularly focused on a large size lead-acid battery. It is capable of providing a bulk constant current with 1/10 C to charge the battery. Accordingly, the charging time can be thus reduced than traditional methods, and the battery temperature can remain no significant change. The experimental results reveal that two series-connected 150AH batteries (24V) can be fully charged using up to 15A within 3 hours. The charging current is soon down to a holding current below about 1A once the full charge is reached. The proposed scheme has been also extended to four series-connected 150AH batteries (48V) charge successfully, and its potential applications in a high power system is thus confirmed.

Keywords: Lead-Acid Battery, Charging System, Multi-state

1. Introduction

Nowadays, the lead-acid battery is widely used in a variety of applications such as electric vehicle, uninterruptible power system (UPS), and emergency power supply, etc. However, some drawbacks, e.g., poor energy density characteristics, long charging time, and short lifetime discourage its further commercial applications. Therefore, the development of optimized algorithm to achieve a rapid charging and prolong the battery lifetime is still an indispensable research issue in industry [1-8].

*Corresponding Author: Cheng Siong Lee
(E-mail:Vincent.CS.Lee@monash.edu).
[1] School of Information Technology, Monash University, Australia

Traditional charge methods either use constant current or constant voltage to charge the battery, or mix these two schemes. However, these methods may suffer from low charge efficiency, over-charge, or long charge time, etc.

Accordingly, a charging method with a negative pulse discharging current was reported [9]–[11]. However, this may cause unnecessary energy consumption and make the charger bulky. In a conventional charger, the well-known two-stage power converter that provides high power factor input and well regulated output exhibits problem such as circuit complexity and high cost. A rapid charger using a single-stage power converter with an energy recovery cell was therefore proposed [12]. This charger can release the stored energy into the batteries during the positive pulse charge period.

Although it can provide high power factor and charging efficiency, a complex control strategy is necessary for performance so that some difficulty may arise to deliver it into a real world. Most recently, a variable frequency pulse charge system (VFPCS) was proposed to improve the battery-charge response [13].

Unfortunately, it was only suitable for small size of battery such as cellular phone charger.

This paper develops a multi-state charge algorithm based on the UC3909 switchmode lead-acid battery charger controller. In Section II, the basic concept of multi-state battery charge is provided. Section III presents an illustrative procedure to design an anticipated charging outcome with the multi-state concept. Experimental results are shown and discussed for details in Section IV. Conclusions are given in Section V.

2. Fundamental Comcept of Multi-state Charge Algorithm

Traditional battery charging modes include: 1.Constant Voltage (CV) charge 2.Constant Current (CC) charge 3.Constant Voltage-Constant Current (CV-CC) charge 4. Pulse charge 5.Positive and

Negative Pulse charge. For details, it is described as follows [14-19].

1). Constant voltage charge mode:

The CV mode is the simplest way to charge the battery. Its charging curve is shown in Fig. 1. It can be seen that the charging current decreases gradually when the battery is going toward fully charged status. This method does not push the battery temperature rising significantly, and no over-charge will occur. However, normally it needs a long charging time, and it may be beyond the rated current at the beginning charge stage.

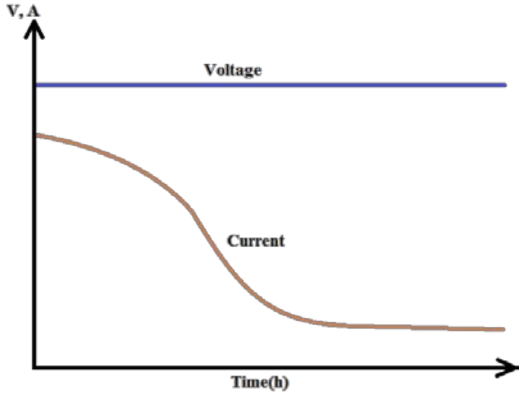

Fig. 1 Charging curve using CV mode

2). Constant current charge mode:

The charging curve using CC is shown in Fig. 2. Based on the CC charge, it is feasible that the charging current can be set under the rated current so that it will not be over the rated limit. On the other hand, the charged voltage will depend on the charging current, and the charge time can be easily estimated. However, the drawback is that it may cause over-charge, and the battery temperature may rise up quickly.

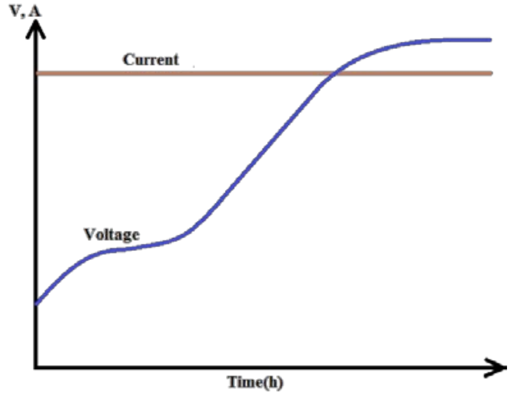

Fig. 2 Charging curve using CC mode

3). Constant Voltage - Constant Current charging mode:

The CV-CC charge mode combines both CV and CC charging method. At the initial charging stage, the constant current is used to charge the battery until the battery voltage reaches over-charged stage or pre-defined voltage. Then, the charging mode will switch to CC one to maintain the battery voltage, avoiding too high voltage. Fig. 3 indicates its charging curve. The advantage of this method is that the charging time can be reduced dramatically. Note that the typical value of maximum charging current is C/10.

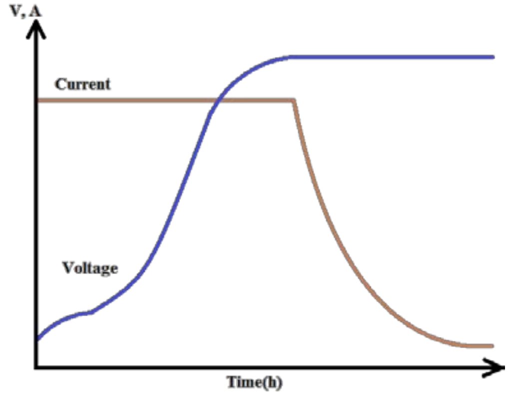

Fig. 3 Charging curve using CV-CC mode

4).Pulse charge mode:

Fig. 4 depicts the profile of pulse charge cycles. Each charging cycle includes “charge” and “rest” stage. In the “charge” period, the battery is charged. In the “rest” period, the battery is at a rest status where the battery has more time to balance the battery chemical reaction. As a result, the battery voltage will become more stable, and its working life can be prolonged. Another advantage is that the charging time can be decreased using a large current which may be over-rated.

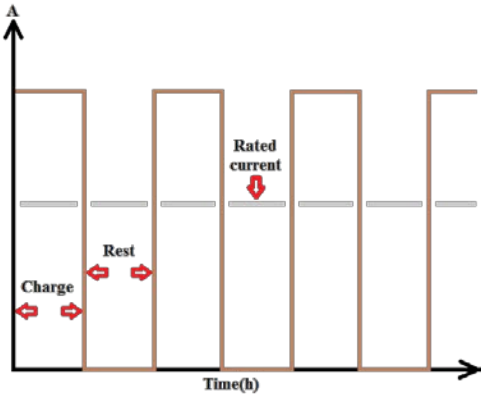

Fig.4 Depict of pulse charge

5). Positive and negative pulse charge:

The concept of applying a short discharge pulse during the charge cycle sometimes referred to as "reflex charging" or "burp charging" started with patents 3,597,673 "Rapid charging of batteries" W. Burkett & J. Bigbee in 1971 and 3,614,583 "Rapid charging of batteries" in 1971 by W. Burkett & R. Jackson. Some of the fast charging systems presently available incorporate negative pulse fast charging algorithms that claim to have great benefits to batteries including reduced recharge time, lower temperature rise, full recharge capabilities, as well as shorter equalization times Also, lots of experimental results support that the negative pulse could eliminate the polarization effective. However, this method may reduce charge efficiency [17-19].

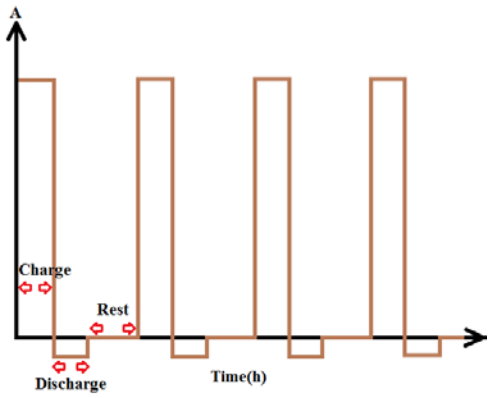

Fig. 5 Depict of positive and negative pulse charge

The best performance of the lead-acid cells can be achieved using a four state charge algorithm. In Fig. 1, the charge states from the first to forth one are trickle charge, bulk charge, over charge, and float charge, respectively. This method integrates the constant current charge to recharge and equalize the lead-acid cells quickly and safely. With the constant voltage, it performs the controlled over-charge and retains the battery's full charge capacity in float mode applications. The carefully tailored charging procedure can maximize the capacity and life expectancy of the battery.

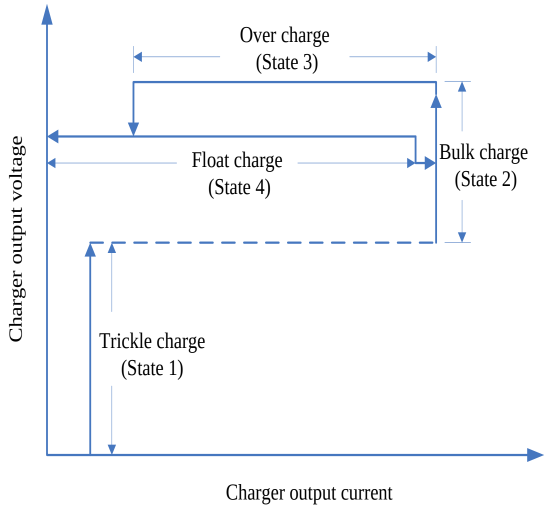

Fig. 6 Four state charge diagram

More details for the four-state charge from Fig. 6 is described as follows, respecting its ideal charge curve, shown in Fig. 5.

State 1 - A pre-charge current (I_T) is applied to a completely discharged battery until a voltage, V_T, is reached. Normally, V_T is set low enough so that if a cell is shorted, no high rate charging will commence.

State 2 - The bulk charge state where the maximum allowable constant current, I_{MAX} , is applied to rapidly charge the battery into the overcharge condition. During this time, the majority of the battery capacity is quickly restored. The bulk charge mode is terminated when the battery voltage reaches the over-charge voltage level (V_{OC}).

State 3 - When the voltage rises past V_{12}, an over-voltage state is entered where the battery voltage now applies a constant level, Voc. The initial current value equals the bulk charge current, and as the battery approaches its full capacity, the charge current will taper off. When the charge current becomes sufficiently low (I_{OCT}), the charging process is essentially finished and the charger switches over to float charge.

State 4 – During this state, the current will be whatever is necessary to maintain maximum capacity. If the battery should become loaded, when the voltage falls below V_{31}, the charger will switch back to State 2 and reapply I_{MAX}, initiating a new cycle.

Some critical points in the four state charge diagram are illustrated as follows.

A: When the input supply power turns on, the battery charges at trickle current (I_T) rate to avoid the possible short circuit. It is in the state 1.

B: The battery voltage (V_{AB}) reaches V_T will enable the driver and turning off the trickle bias output, and then the battery starts to charge at I_{MAX} rate, where it is in the state 2.

C: When the transition voltage V_{12} is reached, and the charger indicates that it is now in the over-charge state, i.e., state 3.

D: When the battery voltage approaches the over-charge level V_{OC}, the charge current will begin to taper.

E: When the charge current tapers to I_{OCT} . The current sense amplifier output, in this case tied to the OC TERMINATE input, goes high. The charger changes to the float state and holds the battery voltage at V_F .

F: Here a load (> I_{MAX}) begins to discharge the battery.

G: The load discharges the battery such that the battery voltage falls below V_{31} . The charger is now in state 1, again.

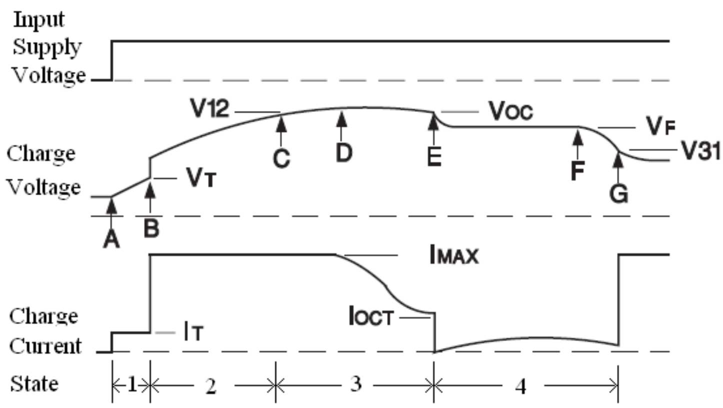

Fig. 7 Four state charge diagram

3. Design of Multi-State Charge Controller

The proposed multi-state charge controller is shown in Fig. 8. The key point to reach the desired charge outcome that matches the four state charge diagram shown in Fig. 7 is to select the appropriate of external parameters such as R_{SM} , R_{DD} , R_{SH} , R_E , R_A , R_C , R_D and R_B .

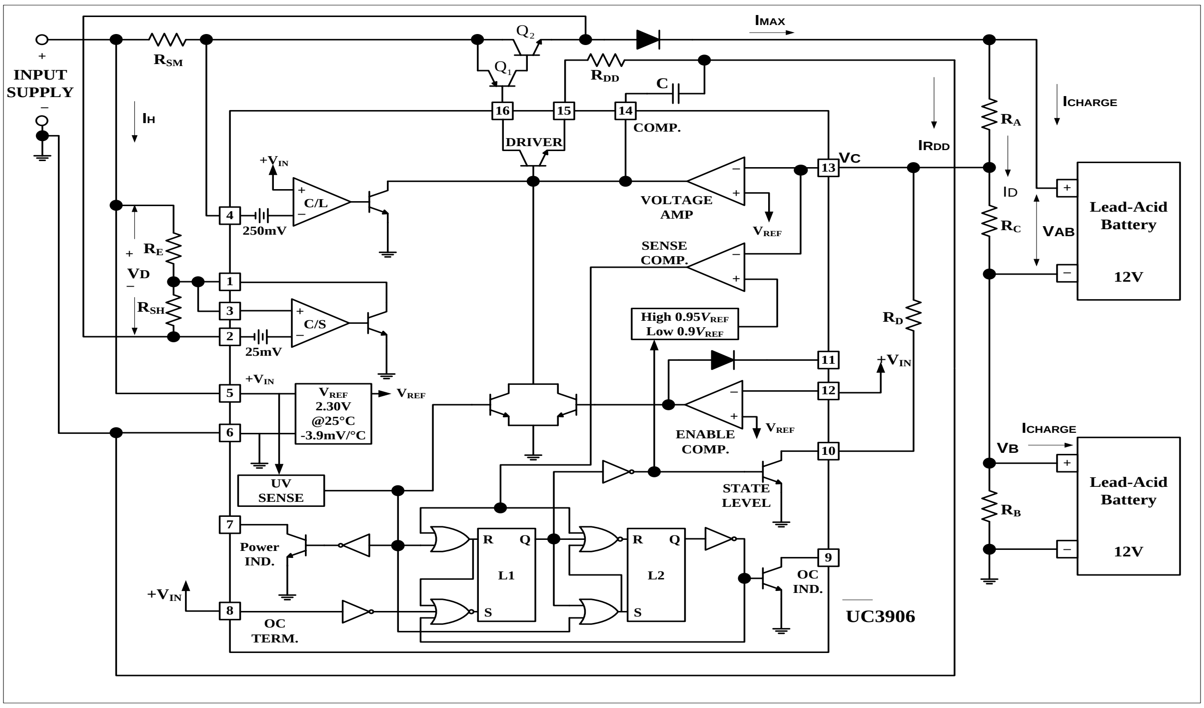

Fig. 8 Hardware of multi-state charge controller

The procedure of the controller design is described as follows:

The maximum allowable current (bulk current) I_{MAX} is handled by the external Darlington circuit (Q_1, Q_2) with the driver supplying base drive to this device. R_{SM} is determined by I_{MAX} as

$$R_{SM} = \frac{0.25}{I_{MAX}} \tag{1}$$

where 0.25V is generated by UC3906.

Therefore, R_{DD} can be calculated as

$$R_{DD} = \frac{V_{IN} - 0.7}{I_{MAX}} \cdot \beta_1 \cdot \beta_2 \tag{2}$$

where $V_{IN} \approx 15V$, and β_1 and β_2 are the current gain of Q_1, Q_2, respectively.

The holding current I_H is to maintain the fully charged battery, and R_{SH} can be obtained as

$$R_{SH} = \frac{0.025}{I_H} \tag{3}$$

where 25mV is generated by UC3906.

When the battery is fully charged, the voltage drop (V_D) between the input supply and battery voltage is about 3V. Consequently, R_E can be obtained as

$$R_E = \frac{V_D - 0.025}{I_H} \tag{4}$$

where $V_D \approx 3V$.

Before the battery voltage (V_{AB}) reaches V_{OC}, the output of SENSE COMP. is set high so that the transistor of STATE LEVEL is turned on. Use the voltage divider rule, and the following relation can be obtained as

$$0.95V_{REF} = \frac{R_C // R_D}{R_A + R_C // R_D} \cdot V_{OC} \tag{5}$$

where $V_{REF} = 2.3V$ is generated by UC3906, and R_D is connected to ground.

The equ.(5) can be rewritten as

$$V_{OC} = 0.95V_{REF}\left(1 + \frac{R_A}{R_C} + \frac{R_A}{R_D}\right) \tag{6}$$

When the battery voltage (V_{AB}) reaches V_{OC}, it begins to enter a float charge state, and at the moment the transistor of STATE LEVEL gets into a cutoff stage. The circuit path of R_D is thus disconnected. Consequently, the equ. (6) can be simplied as

$$V_F = V_{REF}\left(1 + \frac{R_A}{R_C}\right) \tag{7}$$

where the reference voltage with V_C is pulled up to V_{REF} of VOLTAGE AMP from $0.95V_{REF}$ of SENSE COMP.

According to the equ. (7), R_C can be selected arbitrarily, and R_A can be thus determined. As a result, R_D can be found from the equ. (6) as

$$R_D = \frac{0.95V_{REF}R_A R_C}{V_{OC}R_C - 0.95V_{REF}R_A - 0.95V_{REF}R_C} \tag{8}$$

The current I_D that passes through R_A and R_C can be calculated as

$$I_D = \frac{V_F}{R_A + R_C} \tag{9}$$

To keep the same current (I_{CHARGE}) charging the series-connected batteries, the current I_D must pass through R_B. Therefore, R_B can be calculated as

$$R_B = \frac{V_B}{I_D} = \frac{V_F}{I_D} \quad (10)$$

4. Experimental Results

The effectiveness of the proposed algorithm has been tested and verified using both two and four series-connected 12V 150AH batteries. Initially, set INPUT SUPPLY voltage=30V, V_{OC}=14V, V_F=13.8V and I_H =1A for two 12V-battery charge. Also, choose $\beta_1 = 36$, $\beta_2 = 210$. According to the equs. (1)-(10), all external parameter values can be thus obtained as Table 1. The experimental results under different charge currents are shown in Fig. 9- Fig. 13. As can be seen, higher maximum charge current (I_{MAX}) reduces the charge time significantly. In contrast, lower maximum charge current (I_{MAX}) requires more time to achieve the full charge. Obviously, every figure has confirmed a reasonable outcome. For example, 7A charge current shown in Fig. 9 needs more than 8 hours to achieve the full charge. On the other hand, 15A charge current shown in Fig. 13 takes only less than 3 hours to reach a full-charge level. Moreover, in every case the charging current is soon down to the holding current (I_H) once the battery voltage reaches the overcharge (V_F=13.8V).

Table 1 Parameter values

Parameter \ I_{MAX}	15(A)	13(A)	11(A)	9(A)	7(A)
R_B (Ω)	282.2K	282.2K	282.2K	282.2K	282.2K
R_{SM} (Ω)	0.017	0.019	0.023	0.028	0.036
R_{DD} (Ω)	7.2K	8.3K	9.8K	12K	15.4K
R_{SH} (Ω)	0.05	0.05	0.05	0.05	0.05
R_E (Ω)	5.95	5.95	5.95	5.95	5.95

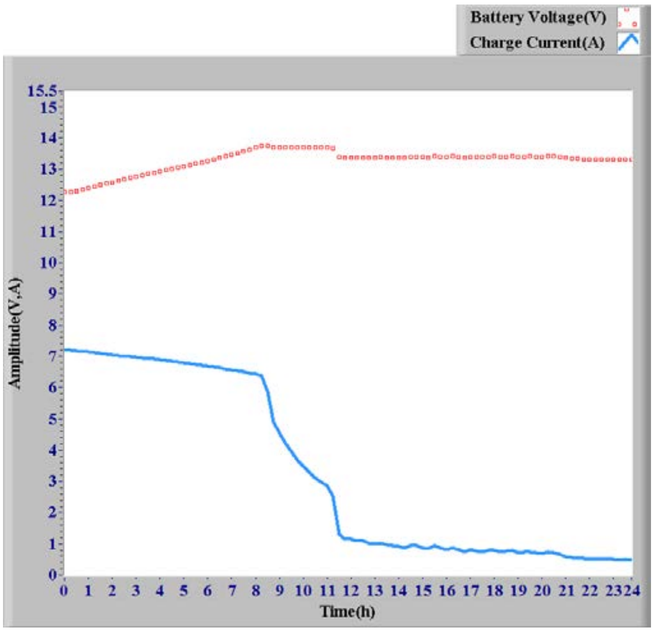

Fig. 9. Charging curves using I_{MAX} =7A, Case 1: I_{MAX} =7A using $R_{SH} = 0.036\ \Omega$.

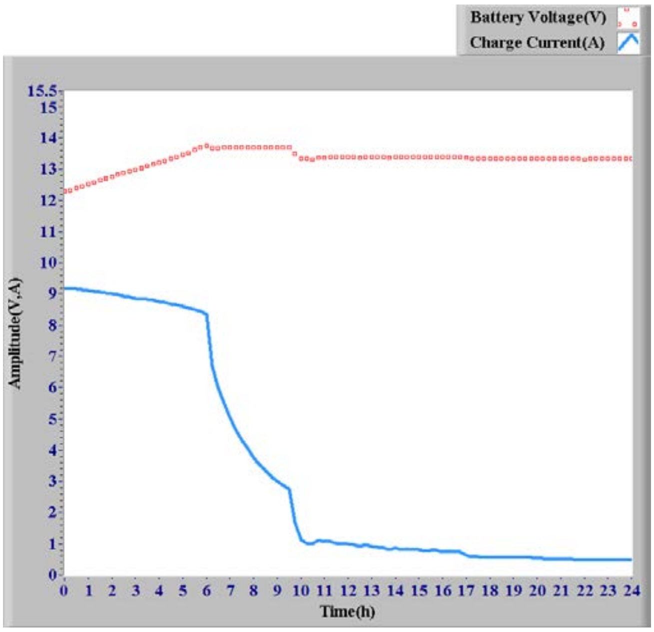

Fig. 10. Charging curves using I_{MAX} =9A, Case 2: I_{MAX} =9A using $R_{SH} = 0.028\ \Omega$.

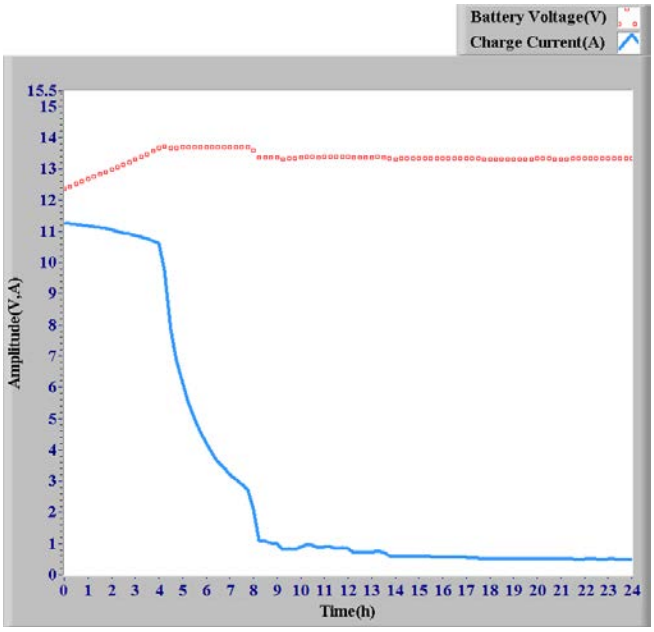

Fig. 11. Charging curves using I_{MAX} =11A, Case 3: I_{MAX} =11A using $R_{SH} = 0.023\ \Omega$.

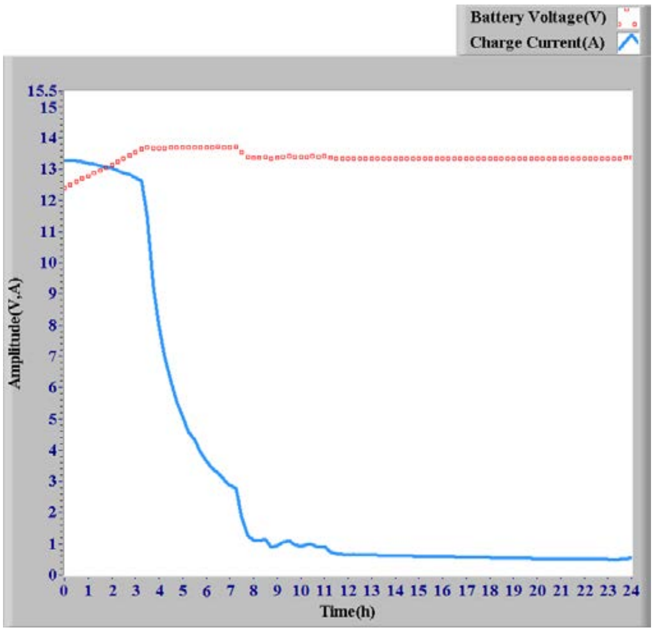

Fig. 12. Charging curves using I_{MAX} =13A, Case 4: I_{MAX} =13A using $R_{SH} = 0.02\ \Omega$.

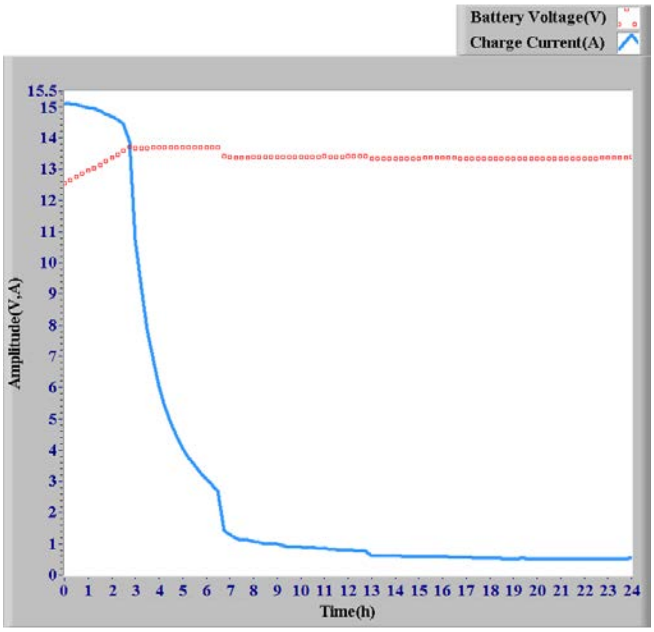

Fig.13. Charging curves using I_{MAX} =15A, Case 5: I_{MAX} =15A using $R_{SH} = 0.017\ \Omega$.

Secondly, set INPUT SUPPLY voltage=60V for four series-connected 12V 150AH batteries (48V) charge, and the other parameters remain unchanged. The experimental results using different charge currents are shown in Fig. 14- Fig. 18. Similarly, the large charge current can reduce the charge time dramatically. For instance, the charging current using I_{MAX} =15A only takes less than 2 hours to reach a full-charge status. On the other hand, the charging current using I_{MAX} =7A requires about 5 hours to achieve the same target.

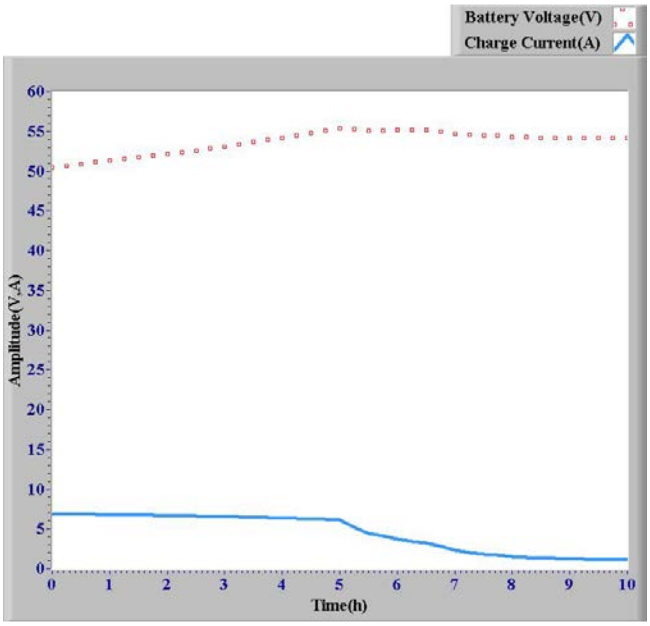

Fig. 14. Charging curves using I_{MAX} =7A, Case 6: I_{MAX} =7A using $R_{SH} = 0.036\ \Omega$.

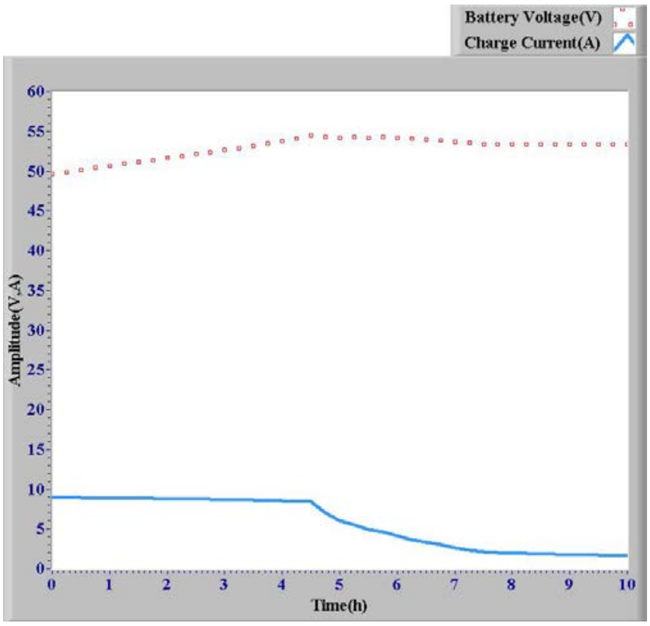

Fig. 15. Charging curves using I_{MAX} =9A, Case 7: I_{MAX} =9A using $R_{SH} = 0.028\ \Omega$.

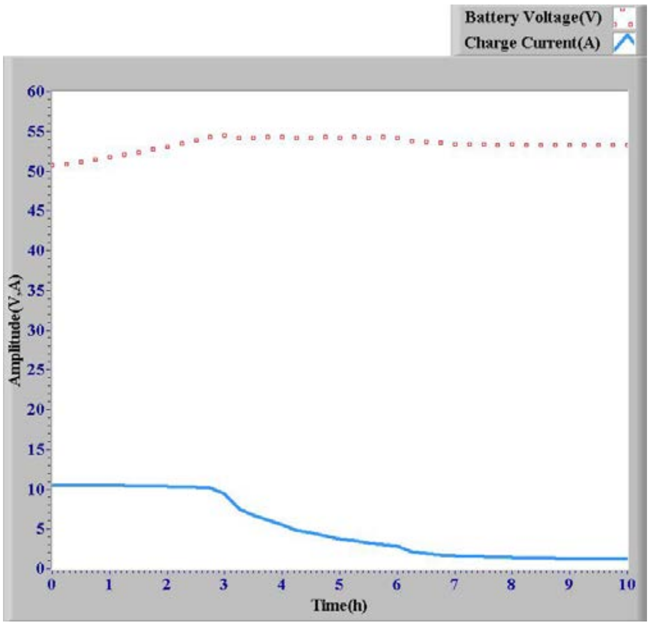

Fig. 16. Charging curves using I_{MAX} =11A, Case 8: I_{MAX} =11A using $R_{SH} = 0.023\,\Omega$.

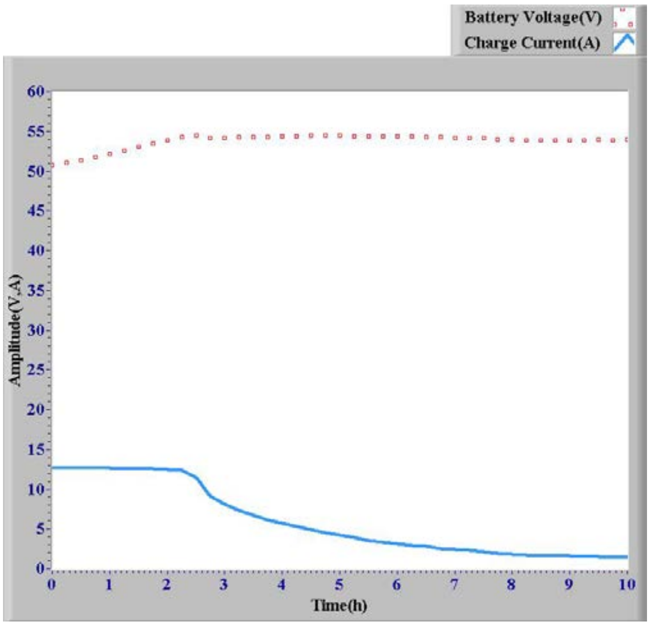

Fig. 17. Charging curves using I_{MAX} =13A, Case 9: I_{MAX} =13A using $R_{SH} = 0.02\,\Omega$.

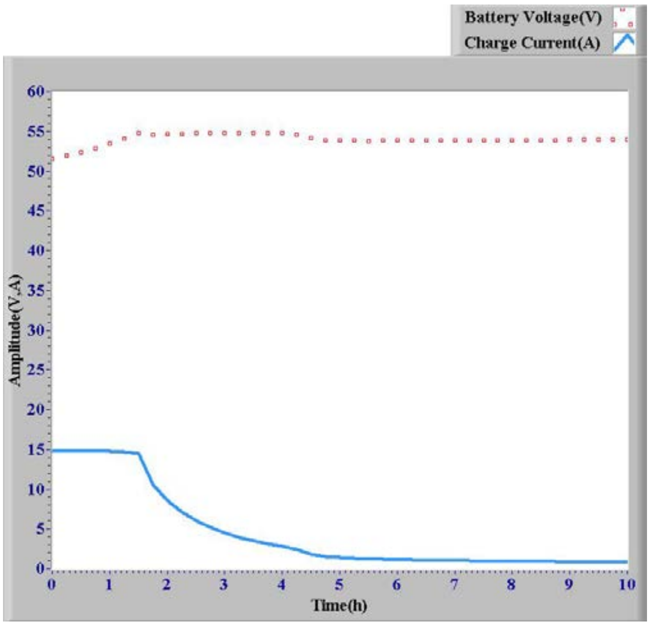

Fig. 18. Charging curves using I_{MAX} =15A, Case 10: I_{MAX} =15A using $R_{SH} = 0.017\,\Omega$.

5.Conclusions

This paper has developed a well-optimized fast charger for a large size of lead-acid battery successfully. The proposed method can fast charge the battery using an appropriate large constant current without significant temperature rising. Once the battery reaches the over-charge state, the charger will soon enter a float-charge state where it remains a small holding current. The experimental results confirm that the proposed charger can complete the charging process within 3 hours for both 24V and 48V battery charge. Unlike the conventional complex control circuit, the proposed scheme is superior in term of simplicity, efficiency and low cost. Based on the design procedure, it can be easily extended to a variety of series batteries charge.

References

[1] Álvarez, J., Marcos, J.; Lago, A.; Nogueiras, A.A.; Doval, J.; Peñalver, C.M., “A fully digital smart and fast lead-acid battery charge system”, IEEE Annual Power Electronics Specialists Conference, Vol. 2, 2003, pp. 913-917.

[2] Yang, Kun; Ouyang, Guangyao; Zhang, Ping; Zhang, Jianping, "Research upon the high-capacity lead-acid battery charge model", 2009 IEEE International Conference on Mechatronics and Automation, 2009, pp. 5079-5083.

[3] Chen, W.L.; Li, J.F.; Huang, B.X., "Design of an energy-saving charge equalization system", Electric Power Components and Systems, Vol. 39, No. 15, 2011, pp. 1632-1646.

[4] Taniguchi, Ittetsu; Kojima, Keita; Fukui, Masahiro, "A practical battery charge/discharge simulator for future embedded systems including smart grids", 2009 International SoC Design Conference, 2009, pp. 173-176.

[5] Li, Wen; Zhang, Cheng-Ning, "Experiments study on charge technology of lead-acid electric vehicle batteries", Journal of Beijing Institute of Technology (English Edition), Vol. 17, No. 2, 2008, pp. 159-163.

[6] Ding, K.; Cheng, K.W.E.; Wang, S.X.; Wang, D.H.; Shi, Zhanghai, "Five-level cascaded multilevel motor driver for electrical vehicle with battery charge management", Australasian Universities Power Engineering Conference, 2008.

[7] Chen, Liang-Rui, "PLL-based battery charge circuit topology", IEEE Transactions on Industrial Electronics, Vol. 51, No. 6, 2004, pp. 1344-1346.

[8] Chen, Liang-Rui, "A design of an optimal battery pulse charge system by frequency-varied technique", IEEE Transactions on Industrial Electronics, Vol. 54, No. 1, 2007, pp. 398-405.

[9] K. C. Tseng, T. J. Liang, J. F. Chen, and M. T. Chang, "High frequency positive/negative pulse charger with power factor correction," in Proc. IEEE PESC'02, Vol. 2, 2002, pp. 671-675.

[10] P. H. Cheng and C. L. Chen, "A high-efficiency fast charger for lead acid batteries," in Proc. IEEE IECON'02, Vol. 2, 2002, pp. 1410-1415.

[11] E. M. Valeriote, T. G. Chang, and D. M. Jochim, "Fast charging of lead-acid batteries," in Proc. ABCAA'94 Conf., 1994, pp. 33-38.

[12] Huang-Jen Chiu, Li-Wei Lin, Ping-Lung Pan, and Ming-Hsiang Tseng, "A Novel Rapid Charger for Lead-Acid Batteries With Energy Recovery", IEEE Transactions on Power Electronics, Vol. 21, No. 3, 2006, pp.640-647.

[13] Chen, Liang-Rui, Young, Chung-Ming; Chu, Neng-Yi; Liu, Chuan-Sheng, "Phase-locked bidirectional converter with pulse charge function for 42-V/14-V dual-voltage PowerNet", IEEE Transactions on Industrial Electronics, Vol. 58, No. 5, 2011, pp. 2045-2048.

[14] Sohn, W.J., and Chainer, T.J.,"Constant-current versus constant-voltage VCM drive analysis ," Magnetics, IEEE Transactions on , Vol.26, May 1990, pp.1217-1224.

[15] B. Dickinson and J. Gill, "Issues and benefits with fast charging industrial batteries," The 15th Annual Battery Conference on Applications and Advances, 1999, pp.223-229.

[16] E. M. Valeriote, T. G. Chang, and D. M. Jochim, "Fast charging of lead - acid batteries," The 9th Annual Battery Conference on Applications and Advances, 1994, pp.33-38.

[17] J. J. Wilkinson, G.A. Covic, "A New Pulse Charging Methodology for Lead Acid Batteries", IPENZ Transactions, Vol. 25, No.1/EMCh, 1998.

[18] Li Siguang Li Siguang, Zhang Chengning Zhang Chengning, Xie Shaobo Xie Shaobo,"Research on Fast Charge Method for Lead-Acid Electric Vehicle Batteries", 2009 International Workshop on Intelligent Systems and Applications, 2009.

[19] M. James, J. Grummett, M. Rowan, J. Newman, "Application of pulse charging techniques to submarine lead-acid batteries", Journal of Power Sources, Vol. 162, Issue 2, Nov. 2006, pp. 878–883.